JOURNAL OF GEOPHYSICAL RESEARCH, VOL. 112, E07002, doi:10.1029/2006JE002862, 2007

On the origin of gypsum in the Mars north polar region

Kathryn E. Fishbaugh,[1] François Poulet,[2] Vincent Chevrier,[3] Yves Langevin,[2] and Jean-Pierre Bibring[2]

Received 16 November 2006; revised 26 January 2006; accepted 29 March 2007; published 13 July 2007.

[1] We describe the distribution and concentration of the largest Martian gypsum deposit discovered to date by the Mars Express OMEGA (Observatoire pour le Mineralogie, l'Eau, les Glaces et l'Activité) imaging spectrometer, its relationship to the late Amazonian-aged north polar dunes in which it is found, and its likely origin. Gypsum has not been discovered anywhere within the north polar region outside of the Olympia Undae dune sea. In the areas of highest gypsum a concentration, 35% pure gypsum grains of a few tens of micrometers in size, mixed with 65% millimeter-sized gypsum grains containing, dark, spectrally featureless inclusions best fit the OMEGA observations. The gypsum-rich dunes contain no significant average albedo, temperature, or morphological anomalies. We propose that water emanating from nearby channels, carved during melting of the polar layered deposits, infiltrated the eastern end of the polar dune sea, percolating through the dunes. Deposits of gypsum resulted from a combination of direct, in situ alteration of sulfide- and high-calcium-pyroxene-bearing dunes and from formation of evaporitic gypsum crystals in the pore spaces of these dunes. This gypsum deposit formed in a unique local environment and is disconnected from sulfate-forming events elsewhere on Mars which are thought to have occurred much earlier, during the late Noachian and Hesperian, by various means. Sulfates have not been discovered in any other collection of dunes on Mars.

Citation: Fishbaugh, K. E., F. Poulet, V. Chevrier, Y. Langevin, and J.-P. Bibring (2007), On the origin of gypsum in the Mars north polar region, *J. Geophys. Res.*, *112*, E07002, doi:10.1029/2006JE002862.

1. Introduction and Background

[2] The Observatoire pour le Mineralogie, l'Eau, les Glaces et l'Activité (OMEGA) on Mars Express has recently detected the largest gypsum deposit on Mars within the Amazonian-aged north polar Olympia Undae sand sea [*Langevin et al.*, 2005] (Figure 1). OMEGA is a visible and near-infrared (NIR) imaging spectrometer (0.35 to 5.1 μm) which has a nominal spatial resolution in the polar regions of a few kilometers per pixel, but data can also be collected at a resolution of $\sim$1 km/pixel. Perhaps the most intriguing aspect of the polar gypsum discovery is the fact that liquid water is needed to form gypsum. While liquid water has carved gullies [e.g., *Malin and Edgett*, 2000] and even outflow channels (review in the work of *Carr* [1996]) during the Amazonian (3.05 bya to present), creation of sulfates is another story. On the basis of the ages of materials revealing rare outcrops of phyllosilicates [*Poulet et al.*, 2005a] and sulfates [*Squyres et al.*, 2004; *Arvidson et al.*, 2005; *Gendrin et al.*, 2005], *Bibring et al.* [2006] have created a preliminary, alteration-based timescale of Mars. Phyllosilicates formed during the "Phyllosian" and sulfates during the "Theiikian," with a boundary between the two epochs at $\sim$4 bya. The late Hesperian to Amazonian (referred to as the "Siderikian") has been dominated by slow weathering, producing anhydrous ferric oxides. Apparently, the discovery of north polar gypsum belies the general aqueous alteration history of Mars inferred from the rest of the OMEGA observations. We will show that geologic conditions unique to the north polar region allowed an apparently anachronous formation of gypsum. First, we describe what gypsum is and in what types of environments it is commonly formed.

1.1. Gypsum and its Occurrence on Mars

[3] Gypsum (hydrated Ca sulfate, $CaSO_4 \bullet 2H_2O$) is a common sulfate-alteration/evaporation product on Earth and is formed in a wide variety of depositional environments [e.g., *Smoot and Lowenstein*, 1991] which lead to its occurrence in a wide variety of settings, for example, in mine waste weathering [*Sracek et al.*, 2004], evaporite assemblages [e.g., *Sinha and Raymahashay*, 2004; *Vysotskiy et al.*, 2004], and hydrothermal deposits [e.g., *Martinez-Frías et al.*, 2004], among many others. This mineral can range from translucent to opaque but is always light in color. Because of its softness (1.5–2 on the Mohs scale), gypsum is easily susceptible to physical weathering.

[4] In White Sands, New Mexico, USA, nearby evaporite deposits have fed a collection of pure, white gypsum dunes which cannot migrate far from their source due to the

[1] International Space Science Institute, Bern, Switzerland.
[2] Institut d'Astrophysique Spatiale, Université Paris-Sud XI, Orsay, France.
[3] W. M. Keck Laboratory for Space and Planetary Simulations, University of Arkansas, Fayetteville, Arkansas, USA.

0148-0227/07/2006JE002862$09.00

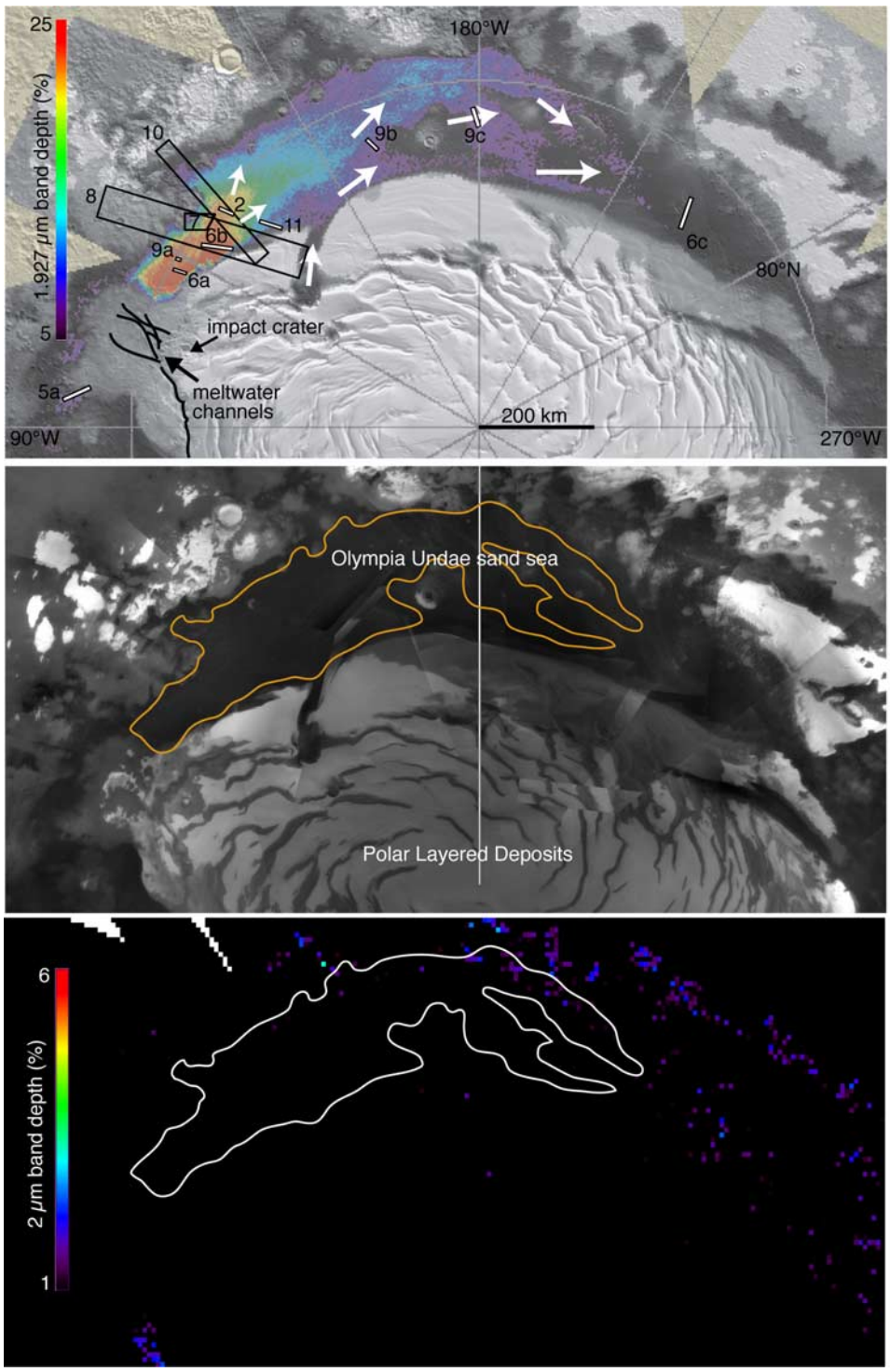

Figure 1. (a) Map of the 1.94-μm absorption feature (diagnostic of gypsum) using the 1.93-μm OMEGA band (modified from the work of *Langevin et al.* [2005]). White arrows indicate main near-surface wind directions as mapped by *Tsoar et al.* [1979]. Meltwater channels are traced in black. Boxes outline locations of other figures. (b) Portion of 64 pixel/degree MOC wide-angle image mosaic. The area containing gypsum is outlined in orange. (c) Map of pyroxene as detected by OMEGA. The pyroxene is identified using the band in the 1- to 1.3-μm range. The area containing gypsum is outlined in white.

physical weakness of the mineral; gypsum sand grains quickly break down into smaller grains which can no longer saltate. The current area of the White Sands dune field is about 710 km^2, much smaller (by an order of magnitude) than the Martian gypsum-rich dune area. However, the White Sands dune field is much younger (~before 5840 year ago to present) than the north polar erg, its source is being depleted, parts of the dune field are still advancing [*Langford*, 2003],

and the size of a sand sea depends on local conditions such as topography, wind speed, and sand supply.

[5] Gypsum also has a low solubility compared to other sulfates (log(K) = −4.58 versus −1.88 for epsomite, $MgSO_4 \bullet 7H_2O$, or −2.19 for melanterite, $Fe^{2+}SO_4 \bullet 7H_2O$ [*Tosca et al.*, 2005]) so any evaporating water containing dissolved gypsum cannot carry it far before the gypsum precipitates.

[6] On Mars, in addition to the north polar deposit, the OMEGA team has tentatively identified gypsum as one constituent in the layered deposits of Juventae Chasma [*Gendrin et al.*, 2005]. The wide range in elevations of sulfate-containing outcrops in Valles Marineris has lead the authors to suggest that the gypsum in Juventae Chasma did not likely originate as an evaporite deposit laid down within a basin, but rather as an alteration-evaporation product; sulfur-bearing water interacted with Ca-bearing minerals, in situ, leaving gypsum as the water evaporated. The MER Opportunity rover has detected concentrations of up to 25 wt.% sulfate salts at Meridiani Planum, which are overlying middle to late Noachian material [*Reider et al.*, 2004; *Squyres et al.*, 2004] and which may have been created by evaporation of fluids involved with weathering of basalts [*Tosca and McLennan*, 2005]. The MER Spirit rover has also detected sulfates within the Hesperian-aged Columbia Hills outcrops, at concentrations of up to 40 wt.% [*Ming et al.*, 2004]. While *Thomas et al.* [1999] have proposed that some bright dunes on Mars, which do not form regional dune seas, may be composed of sulfate grains, the north polar sand sea is the only concentration of dunes on Mars in which sulfates have been definitively identified.

1.2. North Polar Dunes

[7] The north polar sand sea (Olympia Undae), the largest on Mars, consists for the most part of transverse dunes [*Tsoar et al.*, 1979]. Transverse dunes advance perpendicular to the direction of the dune crest by erosion on the windward side and deposition on the leeward side, with one major primary wind direction and other minor wind directions. Where sand supply is relatively low, dunes take the shape of barchans (a crescent-shaped subtype of transverse dune), and where sand supply is higher, they merge into transverse dunes. Longitudinal dunes, which advance along the direction of the dune crest, are also found in rare locations [*Lee and Thomas*, 1995]. *Tsoar et al.* [1979], analyzing Viking images, considered the north polar dunes to be in a young stage of development and to be active based mainly on the following four observations: dune slip faces appear to reverse between images taken during different seasons; horns extending from some barchan dunes extend on top of ephemeral ice; a field of barchan dunes appears to be migrating onto polar ice; and the dunes have a near perfect form, something accomplished on Earth only by active dunes. However, more recent observations indicate that dunes all over Mars may be inactive. No movement of Martian dunes in particular case studies has been observed either between the Viking and Mars Global Surveyor (MGS) missions or during the MGS mission [*Edgett and Malin*, 2000]. Furthermore, the rounded, elongated barchan dunes in the Chasma Boreale region may be indurated, on the basis of both modeling of dune induration and on morphological similarity with terrestrial indurated dunes [*Schatz et al.*, 2006]. Whether or not the dunes within Olympia Undae, in particular, are currently active has not been tested with post-Viking data. Preliminarily, we would suggest that some of the dunes have an eroded rather than fresh appearance indicating inactivity and possible induration (Figure 2). On the other hand, the apparently low thermal inertia of these dunes compared to dunes elsewhere on Mars [*Herkenhoff and Vasavada*, 1999] does not support induration. Regardless of whether or not they are active, the existence of only one crater within the Olympia Undae dunes argues strongly for a late Amazonian age [*Tanaka et al.*, 2005] (0–0.45 By old [*Hartmann and Neukum*, 2001]).

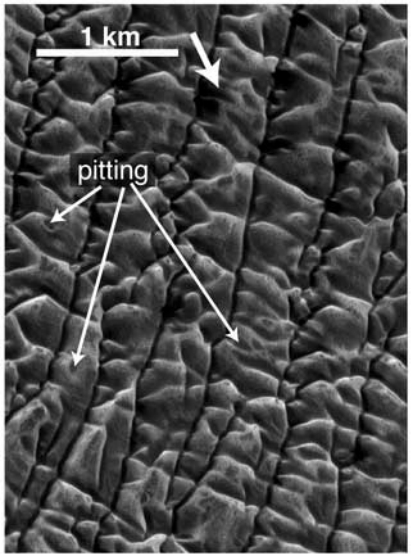

Figure 2. Example of dunes within Olympia Undae that appear eroded and possibly indurated, rather than fresh. Frost highlights features such as pitting on top of the dunes. Portion of MOC image R15/00954. Arrow indicates illumination direction. L_S = 3.00. See Figure 1 for location.

[8] These young dunes compose some of the darkest materials on the planet [*Thomas and Weitz*, 1989] (TES lambert broadband albedo of ~0.12 (J. Bandfield, personal communication Infrared Thermal Mapper (IRTM)) and Viking, 2007 albedo of 0.1–0.2 [*Paige et al.*, 1994]). In Mars Odyssey Thermal Emission Imaging System (THEMIS) data, the dunes have a color similar to the polar basal unit [*Fishbaugh*, 2005], which lies stratigraphically beneath the polar layered deposits (PLD) and from which the dune-forming material is believed to have eroded [*Byrne and Murray*, 2002; *Edgett et al.*, 2003; *Fishbaugh and Head*, 2005].

[9] While a thorough compositional study of the Olympia Undae dunes, in particular, has not yet been produced, the polar sand seas display the best example of the MGS Thermal Emission Spectrometer (TES) type II terrain (J. Bandfield, review's comments), which is generally acknowledged to be a surface dominated by intermediate plagioclase and high-Si glass with perhaps some pyroxene (OPX or CPX) [*Bandfield*, 2002]. The plagioclase and high-Si glasses are transparent in the NIR wavelength region covered by OMEGA.

[10] Besides gypsum, OMEGA has preliminarily detected low concentrations of oxides and/or olivine (difficult to distinguish), areas with no clear spectral absorption features,

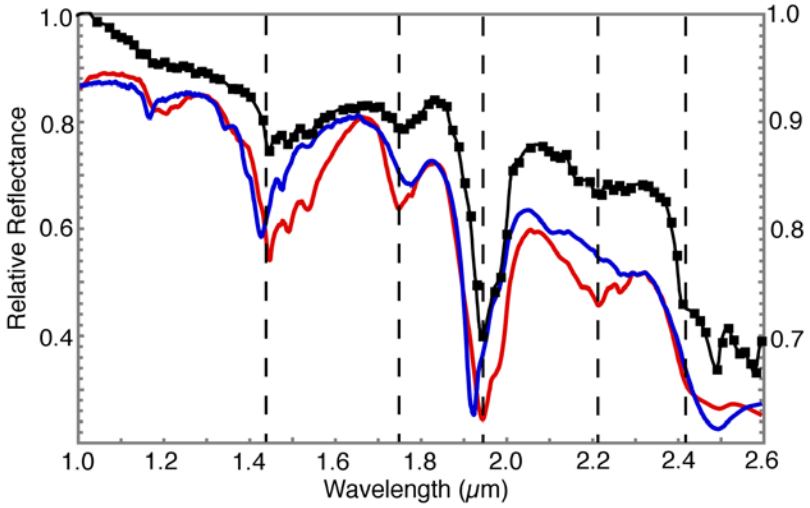

Figure 3. Comparison of the spectral signature of the gypsum-rich region with spectral libraries. The black spectrum is a spectral ratio at L_S 136.2° between the region at 240.2°E, 79.9°N which presents the largest hydration signature at 1.94 μm and a region at 244°E, 77°N where this signature is much weaker. The squares correspond to the spectral sampling. The absorption features are strongly diagnostic of calcium sulfates. The blue spectrum corresponds to bassanite ($CaSO_4$, 0.5 H_2O), and the red spectrum corresponds to gypsum ($CaS0_4$, $2H_2O$) from the USGS spectral library [*Clark et al.*, 1993]. The relative reflectance scale for the Mars spectra (right) has been expanded with respect to that of the laboratory spectra (left). The position and fine structure of the 1.445-μm absorption, the position of the 1.75-μm absorption, the position and shape of the 1.945-μm absorption, the presence of an absorption at 2.21 μm, and the sharp decrease in reflectance at 2.4 μm provide a highly consistent and unambiguous identification of gypsum with respect to less-hydrated forms of calcium sulfates.

and the presence of unidentified, hydrated minerals in most of the area north of 60°–60°N [*Poulet et al.*, 2005b]. Small amounts of pyroxene, mostly outside the gypsum-rich area (Figure 1c), and polyhydrated sulfates are also present, the latter being confined to small, isolated dune patches to the east of the main dune sea margin. While pyroxene and hydrated sulfates have been detected within north polar dunes, these minerals are not found in dunes elsewhere on Mars.

[11] *Herkenhoff and Vasavada* [1999] conjectured that the Olympia Undae dunes may be composed of filamentary sublimation residue (FSR) particles, ash and dust held together in sand-sized aggregates formed during sublimation, in this case, of the polar layered deposits (PLD). This hypothesis was especially attractive when it was thought that the source of dune material was the sediments within the PLD [*Thomas and Weitz*, 1989] rather than within the polar basal unit; if particulates within the PLD originated as airborne material, then sand-sized grains could not be eroding from these deposits to form dunes. However, the polar basal unit, discovered only with the advent of MGS Mars Orbiter Camera (MOC) data, is thought to be composed, at least partially, of sand-sized particles so that invoking FSRs is no longer necessary to explain the presence of the dunes. Nevertheless, the apparently low thermal inertia has yet to be explained unless it is due to previously unconsidered factors such as the effects of slope on apparent temperature. It is within this unique sand sea that the OMEGA instrument has discovered the largest gypsum deposit on Mars.

1.3. Previous Studies Concerning North Polar Gypsum

[12] *Langevin et al.* [2005] have used OMEGA data to identify gypsum within Olympia Undae mainly by its absorption feature at 1.94 μm, which is associated with several features typical of gypsum in the 1- to 2.5-μm range. By taking a ratio of a spectrum from gypsum-rich dunes to a spectrum of gypsum-poor dunes, the authors emphasized that the resultant absorption features much more closely match those of pure laboratory gypsum than those of other, less-hydrated calcium sulfates, such as bassanite (Figure 3). We discuss the concentrations and distribution of this gypsum deposit in section 2.

[13] While not discussed in detail, *Langevin et al.* [2005] favored the following two possible origins for this deposit, acting either alone or in combination: interaction of Ca-rich minerals with H_2SO_4-bearing snow resulting from extended volcanic activity nearby or formation as an evaporite deposit within a pool produced by outflow from the PLD (either the current or any previous PLD). As pointed out by the authors themselves, a major difficulty with the first hypothesis is the small area to which the gypsum is confined. One would expect larger-scale alteration of more circumpolar materials (with the same Ca-rich composition) unless this acidic snow somehow fell only in a confined area.

[14] More recently, in a preliminary study, *Tanaka* [2006] has suggested that the north polar gypsum deposit resulted from circulation of hydrothermal groundwater associated with magmatism at Alba Patera during the early Amazonian (~1.75–3.05 bya) [*Hartmann and Neukum*, 2001]; later, eolian activity excavated this deposit. Expulsion of groundwater from graben elsewhere on Mars, in the Elysium and Tharsis regions, has formed such features as major channels and lahar deposits (which are not observed in the north polar region) but no exposed sulfate salt deposits [*Christansen*,

1989; *Tanaka and McKinnon*, 1989; *Skinner and Tanaka*, 2001; *Russell and Head*, 2003]. Timing could also present a problem in this scenario. Either the gypsum was created before the dunes, has been exposed by wind erosion only at the locations where dunes now exist (i.e., nowhere else in the northern plains), and is now incorporated within the dunes or the dunes are actually early Amazonian in age, belying their crater-counting age.

1.4. Goals of This Study

[15] The north polar gypsum deposit is unique on Mars in comparison to other sulfate deposits in terms of albedo (relatively dark), spectral signatures (deep versus shallow), morphology (dunes versus outcrops), and exposed area (much larger). The main goal of this study is to investigate the origin of the north polar gypsum using mainly MGS MOC images, Mars Odyssey THEMIS data, MGS Mars Orbiter Laser Altimeter (MOLA) data, and OMEGA data. The achievement of this goal involves characterization of the geologic setting of the gypsum deposit, describing the relationship of the gypsum with the dunes in which it is found, tentatively identifying the source of Ca^{2+} and SO_4^{2-} needed to create the gypsum, and finally building a description of the geologic sequence of events which lead to its formation. While we concentrate on the OMEGA observations of this gypsum deposit and how this unique deposit fits into the local geology, we also perform preliminary geochemical analysis.

2. Observations in the North Polar Region

2.1. Gypsum Concentrations

[16] In Figure 1a, we map the strong 1.94-μm gypsum absorption feature using the 1.93-μm OMEGA channel in order to reduce contamination by atmospheric CO_2; excluding the grain-size effect (explained below), it is essentially a map of gypsum concentration. As discussed in section 1.3, this gypsum has been identified by spectral ratios so that, while a strong absorption feature at 1.94 μm is also diagnostic of other sulfates and clays, in this region, it is diagnostic of gypsum (Figure 3). The reflectance at the bottom of the gypsum band, at locations of maximum concentration (red in Figure 1a, centered around 160°W), is nearly 25% lower than the continuum, half the value for pure, laboratory gypsum powder, grading to ~5% band strength at the low concentrations toward the west (purple in Figure 1a). The detection limit of the OMEGA instrument, in terms of abundance, depends on grain size as follows: ~15 vol.% for grain size $\leq$5 μm and $\leq$5 vol.% for grain sizes $\geq$10 μm [*Poulet et al.*, 2007]. This means that OMEGA can easily detect small amounts of sand-sized (hundreds of microns) gypsum but cannot so easily detect small amounts of fine-grained gypsum (a few microns).

[17] The extraction of quantitative information about composition and physical state (for example, the volume percentage of gypsum) from spectra requires accurate models of radiative transfer within the surface materials. In this work, we use the approach adopted by *Shkuratov et al.* [1999]. This approach, on the basis of approximation of geometrical optics (as is the more familiar Hapke model [*Hapke*, 1981]), is used to transform optical constants into a reference spectrum and provide the spectral albedo of powdered surfaces. The compositional model for this study must satisfy the following two major constraints: the observed low albedo of the gypsum-containing dunes and the observed gypsum band depths. We use the gypsum optical constants derived by *Roush et al.* [2006]. Dark and spectrally featureless (DSF) grains act as darkening agents [*Poulet et al.*, 2003; *Poulet and Erard*, 2004].

[18] For an intimate ("sand") mixture wherein gypsum sand grains are mixed with DSF grains, the best fit to our compositional model (Figure 4a) is as follows: 55% DSF mixed with 45% gypsum. We use a grain size of 100 μm–1 mm for the gypsum component, and a few tens of microns for the DSF component. Note that the grain size of the DSF (and thus the abundance) is not well constrained because there is no absorption feature. Increasing the grain size will decrease the abundance of the DSF phase so that the 55% reported above corresponds to an upper limit. Estimates of average Martian dune grain size range from 500 ± 100 μm [*Edgett and Christensen*, 1991] to several millimeters [*Christensen et al.*, 2003]. *Edgett and Christensen* [1991] calculated a minimum size for saltation of 210 μm; hence most of the gypsum grains within the range of sizes we use would be theoretically able to saltate. However, an intimate mixture is inconsistent with TES thermal infrared data which do not indicate a presence of large amounts of coarse-grained oxides.

[19] In addition to common intimate mixtures, we can test an "intramixture" model in which larger grains house smaller inclusions [*Poulet and Erard*, 2004]. If, during its precipitation, the gypsum incorporated grains of darker material, such as DSF, drastic effects both on albedo and band depth would ensue. In this case (Figure 4b), we find that 35% pure gypsum grains of a few tens of microns in size mixed with 65% millimeter-sized gypsum grains, contaminated by small inclusions of DSF, best fits the OMEGA observations. These grain sizes are averages from a distribution of possible sizes. The millimeter size is required to fit the deep absorption features of gypsum, while the smaller size is mostly necessary to increase the overall albedo. Within the saltating intramixture, there should be almost no albedo contrast since the dark inclusions considerably lower the apparent albedo of the surrounding gypsum matrix. Indeed, an intramixture provides a better fit to our compositional model than does an intimate mixture (Figure 4b). This type of mixture presents several major additional advantages as follows: it is consistent with the presence of a large component of spectrally featureless material, inferred by OMEGA observations to exist within the dune sea; oxides, which are dark and spectrally featureless, are a significant secondary phase expected from the weathering of Fe-bearing high-calcium pyroxene (HCP) during the formation of gypsum (as explained in section 3.2.2); and the intramixture model appears to be more consistent with TES thermal infrared spectra, because the derived abundance of oxides is under the detection limit of TES (TES has not observed oxides in this dune sea).

2.2. Gypsum Distribution

[20] The area of highest gypsum concentrations lies at the eastern edge of the main north polar dune sea, covering an area of ~7500 km^2 (Figure 1a). This area

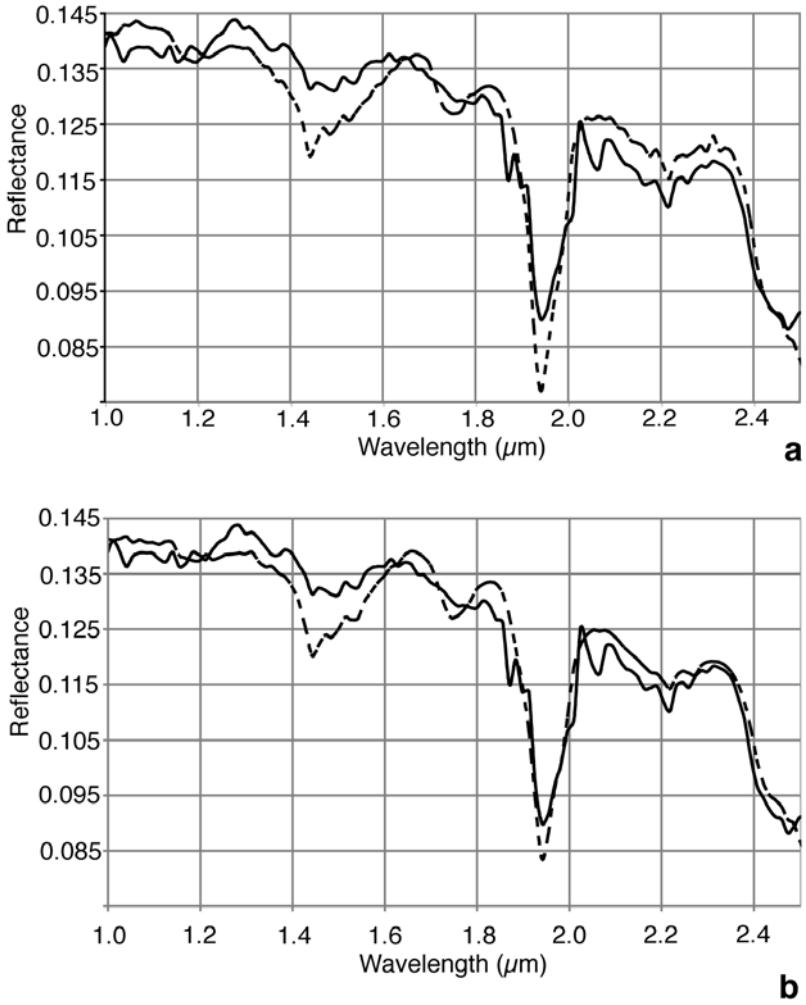

Figure 4. Comparison of OMEGA spectrum from the gypsum-rich dune region (solid line) with (a) a spectrum generated by our intimate mixture model (dashed line) and with (b) a spectrum generated by our intramixture model (dashed line). The intramixture model proves a better fit to the OMEGA data.

of the sand sea is geologically different from the westernmost portions because small, sinuous valleys terminate just to the southeast (outlined in Figure 1a). Gypsum concentration decreases toward the west, in the same direction as the main near-surface winds as mapped by *Tsoar et al.* [1979] using dune morphology. Beyond ~210°W, little to no gypsum appears, though the main dune sea extends to ~240°W.

[21] At first glance, the gypsum in Figure 1 appears to be confined to the main dune field (low-albedo area labeled in Figure 1b). Indeed, this observation is borne-out within higher-resolution MOC images. Other than small hills within the dune sea and the extreme eastern edge of the dune sea where dune coverage is more sparse, we find almost no areas where gypsum exists without dunes. Even the small gypsum patches outside of the main dune field, to the east of the high-concentration area, lie within dunes (purple patches in Figure 1a, Figure 5). No gypsum has been detected within the polar cap or circumpolar materials.

2.2.1. Gypsum Within the Dunes

[22] Further investigation of the relationship between the Olympia Undae dunes and the gypsum reveals that there are

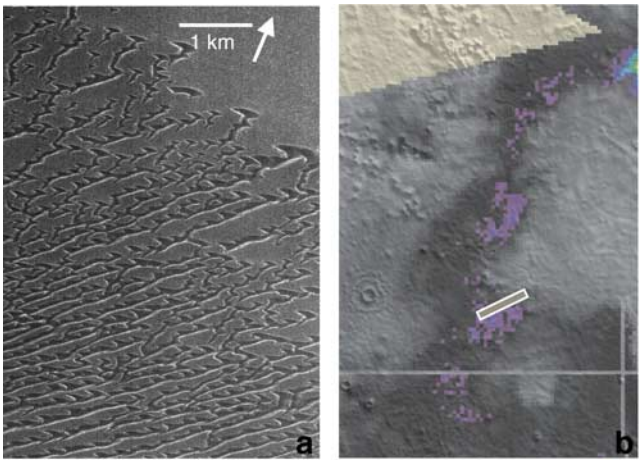

Figure 5. (a) Example of a small patch of gypsum lying within dunes outside of the main north polar dunes field (portion of MOC image R14/00210, arrow indicates illumination direction). (b) Location of MOC image with respect to the gypsum concentration map. See Figure 1 for context.

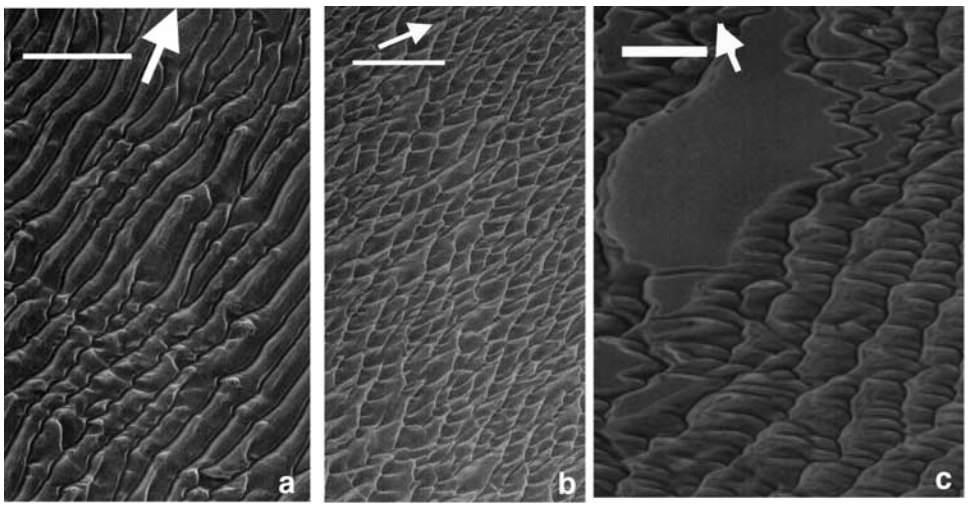

Figure 6. Examples of dunes with different gypsum concentrations. (a) Example of complex linear dunes within the highest gypsum concentrations. Note that all examples were taken during northern winter and therefore may contain frost. Portion of MOC image R13/03611 (L_S = 338.14°). (b) Example of complex transverse dunes within the highest gypsum concentrations. Portion of MOC image R14/00532 (L_S = 344.68°). (c) Example of complex transverse dunes which contain no gypsum. Portion of MOC image R14/00706 (L_S = 345.28). Arrows indicate illumination direction. Scale bars are 1 km. See Figure 1 for locations. There is apparently no correlation of gypsum concentration with dune morphology. Additionally, there appears to be no surficial crusts or ubiquitous loose deposits of bright gypsum on the dunes with high gypsum concentrations.

few anomalous characteristics of the gypsum-bearing dunes in comparison to those in which gypsum has not been detected. In MOC images, we find no correlation of gypsum concentration with dune morphology. Both gypsum-rich and gypsum-free areas contain a variety of barchan and transverse dune morphologies (Figure 6). This is not entirely unexpected as dune morphology on Earth generally has no correlation with sand composition. The gypsum dunes of White Sands, New Mexico comprise the following four major dune types whose morphologies are related to sand supply and wind direction, not to their gypsum content: parabolic dunes, barchan dunes, transverse dunes, and dome-shaped dunes [e.g., *McKee*, 1966]. Additionally, the area of highest gypsum concentration has only a slightly higher albedo on average (0.16) than the dunes that lack gypsum (0.14), and no apparent color anomalies manifest themselves in THEMIS images (Figure 7). THEMIS IR data indicate no temperature anomalies in the gypsum area either (Figure 8).

[23] In MOC images taken during northern summer, we have found instances of bright patches of material, which have collected mostly in low areas between dune crests and are scattered throughout the area covered by gypsum-bearing dunes, though not ubiquitously (Figure 9). These patches have not yet been found (in MOC images) within the western portion of the dune sea in which gypsum has not been detected. However, we have observed bright patches in a Mars Reconnaissance Orbiter (MRO) High Resolution Imaging Science Experiment (HiRISE) image within the dune field bordering the mesa near the mouth of Chasma Boreale. No gypsum has been detected here by OMEGA, but perhaps the grain size is too fine and the amounts too low (in section 3.4.2, we discuss gypsum in association with Chasma Boreale). The HiRISE image

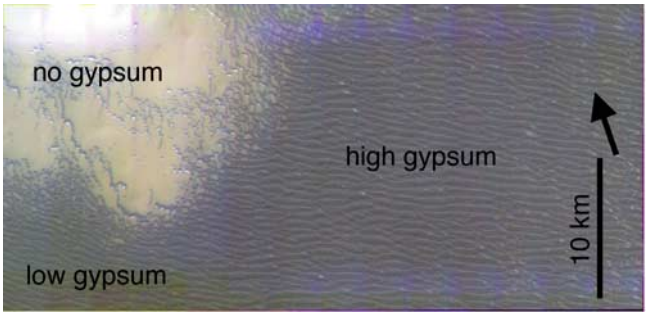

Figure 7. The gypsum-rich dunes exhibit no color anomalies in relation to the low-gypsum dunes. The gypsum-free area is reddish relative to the bluish dunes, likely due to the presence of dust. THEMIS false color visible image V04067010. Blue = Band 1 (0.425 μm), Green = B2 (0.540 μm), and Red = B3 (0.654 μm). L_S = 94.885. Arrow indicates illumination direction. See Figure 1 for image location.

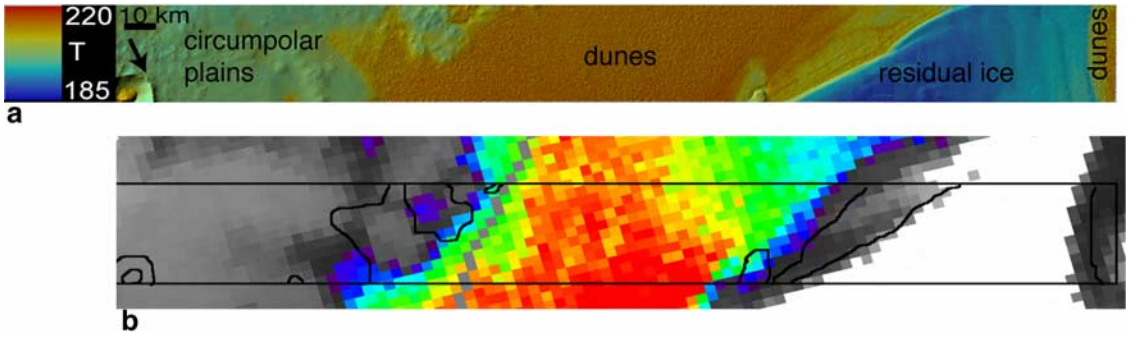

Figure 8. (a) Derived brightness temperature for Band 9 of THEMIS infrared image I04067009 (L_S = 94.885; local time = 3.382; incidence angle = 71.256°). Projected temperature data courtesy THEMIS Processing Web Interface (THMPROC): http://thmproc.mars.asu.edu. Arrow indicates illumination direction. See Figure 1 for location. While brightness temperature is not equal to the physical temperature, it is a reasonable approximation since most natural surfaces have an emissivity close to 1 at IR wavelengths. In this example, no significant temperature anomalies are apparent within the gypsum-rich dunes. (b) Portion of the gypsum concentration map shown in Figure 1 with the main features of the THEMIS image in Figure 8a outlined for reference.

(Figure 9d) reveals eolian ripples on the surfaces of the patches; this, along with the summer season in which this image and the MOC images were taken, make it unlikely that the patches are composed of frost. It may also be possible that this bright patch observed by HiRISE is not the same type of bright patch observed by MOC within the main polar dune sea. Note that these patches are different from a few exposures between dunes (in the eastern, gypsum-free portion of the dune sea) of bright substrate, which is often characterized by polygons.

[24] While OMEGA cannot resolve the bright patches, the MRO Compact Reconnaissance Imaging Spectrometer for Mars (CRISM) can. While no data or publications have yet been released concerning these bright patches, a recent press release concerning one CRISM image (13 December 2006, http://www.nasa.gov/mission_pages/MRO/multimedia/pia09094.html) indicates that the bright patches are relatively low in gypsum compared to the dunes themselves and that the crests of the dunes exhibit the highest gypsum concentrations. It is yet to be seen whether or not these observations are representative of the entire gypsum-rich area, but we suspect that grain-size effects similar to those of OMEGA data play a role in the relatively low gypsum concentration of the patches; the possibly small grain sizes within these patches may make detection of gypsum more difficult. Additionally, underlying material may outcrop within the bright patches, creating a mixed spectral signature.

[25] Figure 10 displays the gradual transition from high gypsum to lower values to the surrounding gypsum-free plains in the context of a THEMIS IR image. Again, the gypsum-rich areas lie almost exclusively within dune-covered regions. Transitions from high- to low-gypsum

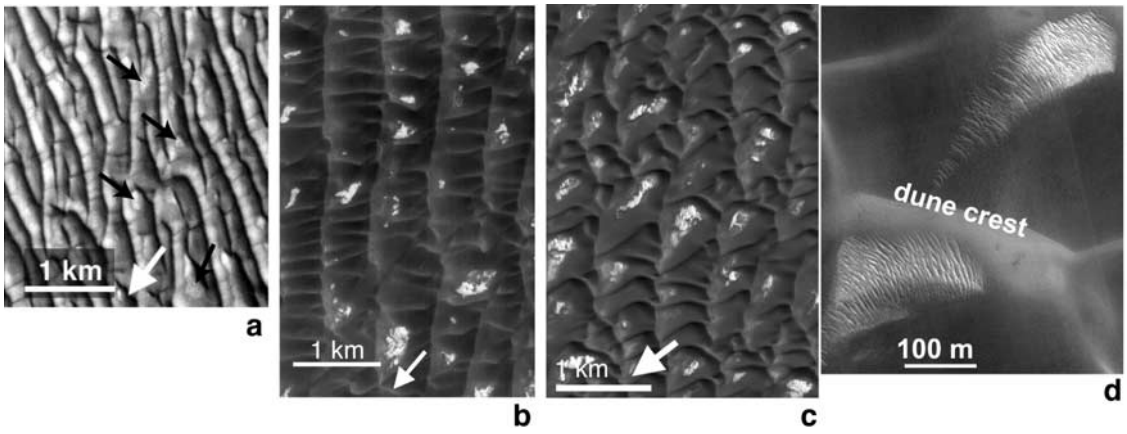

Figure 9. Examples of dunes with associated bright patches which may be gypsum. Both images were taken during northern summer. (a) Portion of MOC image M01/05259, L_S = 147.21°. Black arrows point out examples of the bright patches. White arrow indicates illumination direction. (b) Portion of MOC image M02/04467, L_S = 161.91°. Arrow indicates illumination direction. (c) Portion of MOC image E01/00916, L_S = 117.32°. Arrow indicates illumination direction. See for Figure 1 for image locations for Figures 9a, 9b, and 9c. (d) Portion of HiRISE image TRA_000861_2580_RED, illuminated from the lower left, L_S = 114.9°. This image lies within the dune field bordering the mesa beyond the mouth of Chasma Boreale (see Figure 14).

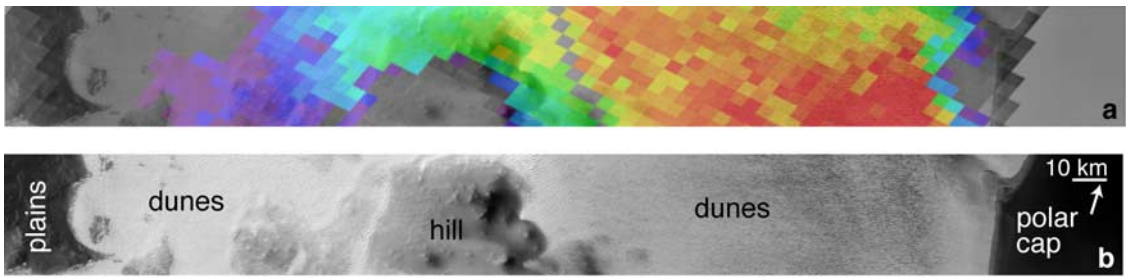

Figure 10. Illustration of the regional, morphological context of the gradual transition from high gypsum concentrations to low concentrations to surrounding gypsum-free plains. (a) Portion of the gypsum map from Figure 1a overlying THEMIS IR image in Figure 10b. Note that OMEGA data and THEMIS data have not been perfectly coregistered. (b) Portion of THEMIS IR image I03750002. Arrow indicates illumination direction. See Figure 1 for location. The changes from high gypsum concentrations to lower concentrations do not appear to be controlled by (i.e., do not mimic) changes in regional morphology.

concentrations and between gypsum-containing and gypsum-free areas do not express themselves in the regional morphology. Put another way, regional morphologic variations do not appear to have affected gypsum concentration. Note that small amounts of gypsum appear to be associated with part of a hill in the middle of Figure 10. Given that the appearance of any gypsum anywhere other than within dunes is a quite rare occurrence, we speculate that the gypsum, apparently associated with this hill, is due to the imperfect registration of OMEGA data to MOLA data. Note that most of the hill is entirely gypsum free.

2.2.2. Gypsum in the Basal Unit?

[26] Several authors have identified the north polar basal unit, lying stratigraphically beneath the polar cap, as the main, if not sole, source for the north polar sand sea [*Byrne and Murray*, 2002; *Edgett et al.*, 2003; *Fishbaugh and Head*, 2005]. High-resolution OMEGA data (at 1-km pixel) reveal a gap between areas containing high gypsum con-

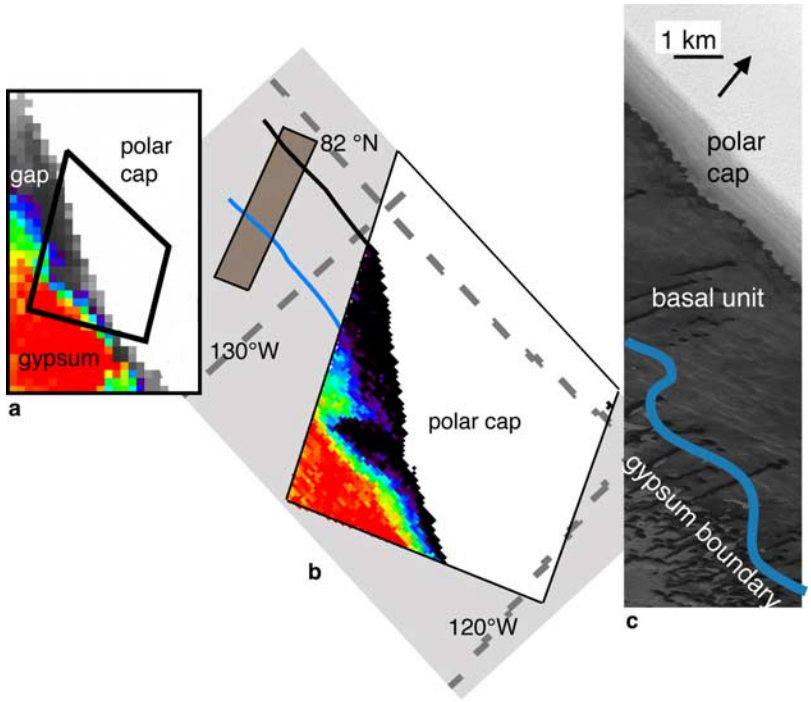

Figure 11. Illustration of the lack of gypsum in the north polar basal unit (main source of the sand sea). (a) Portion of normal-resolution gypsum map in Figure 1 as context. (b) High-resolution OMEGA data (1 km/pixel), spanning the polar cap margin, a gap in gypsum, and part of the highest gypsum concentrations. Grey area indicates "no data." Rectangle shows location of full-MOC image on the right. No MOC images were available exactly in the location covered by the high-resolution OMEGA data. (c) Portion of MOC image E02/01976 showing that the gap in gypsum corresponds with the presence of the dark, layered north polar basal unit. Arrow represents illumination direction. See Figure 1 for MOC image location.

centration and the PLD (Figure 11). This gap is occupied by a dark, layered material previously identified as part of the basal unit. Thus it appears that the basal unit, while being the source for the majority of the dune material, is probably not the source for the gypsum within the dunes. This observation can be tested further after the collection and better georeferencing of more high-resolution OMEGA data as well as dedicated observations by CRISM, which has a spatial resolution of $\geq$18 m/pixel.

3. Discussion

3.1. Association With Sand Dunes

[27] Several observations indicate that the bulk of the observed gypsum consists of sand-sized grains (with dark inclusions) which are incorporated into dunes rather than forming surficial crusts or fine-grained deposits. (1) No significant, ubiquitous color, thermal, or average albedo anomalies are associated with the gypsum-bearing dunes. (2) Gypsum has been detected almost exclusively within dunes. (3) Gypsum concentration decreases westward, in the same direction as the main near-surface winds (see Figure 1). It appears that the decreasing amount of gypsum in this direction is partly due to the fact that most of the gypsum-containing dunes haven't migrated that far.

[28] There are several reasons why gypsum would be detected within sand dunes. (1) The existence of a collection of dunes indicates that deposition of wind-blown material is taking or has taken place there. In areas without dunes or other sediment deposits, wind-blown material is either being net removed or just not being deposited. Gypsum would be expected to accumulate in an area of net deposition (for example, a dune sea) rather than in an area of net erosion or nondeposition. (2) The saltation process would clear the surface of fines, removing any dust which could mask a gypsum signature. Of course, this is operating in the polar dune sea only if the dunes are active. (3) At the wavelengths used to detect gypsum, OMEGA is most sensitive to sand-grain-sized particles. Small amounts ($\sim$15% maximum) of undetectable, finer-grained gypsum may exist elsewhere. (4) As discussed below, formation of gypsum would most likely occur where Ca-bearing sediment (the dunes; see section 3.2.2) is present and where a large exposed surface area makes alteration to gypsum easier (within collections of loose sand grains).

[29] Given the difference in hardness of the gypsum and DSF components, a physical segregation between grains mostly composed of gypsum and of mostly DSF and other components should occur due to the saltation process. The farther the dunes migrate, and hence the farther the individual sand grains saltate, the more the soft gypsum would break down. Erosion during saltation would reduce the size of the gypsum particles until they become too small to saltate. Over time and saltation distance, more and more gypsum would end up as fine-grained deposits blown by the wind and collecting in interdune spaces and the leeward side of dunes but would not be mixed-in with the saltating dark sand. If the dunes eventually become inactive, then fine-grained gypsum could also collect on dune crests. The eolian-rippled, bright patches (that are not exposures of polygonally-patterned underlying material) observed in MOC images scattered throughout the gypsum-rich dunes may comprise the fine-grained (tens of microns), pure gypsum component of our intramixture and the gypsum which has been mechanically weathered during saltation. Since these bright patches do not markedly increase in spatial density with distance from the highest gypsum concentrations, the decrease in gypsum concentration toward the west probably has more to do with the gypsum not having yet saltated that far than with a decrease in grain size lessening the gypsum signature.

3.2. Source of the Ingredients Necessary to Form Gypsum (Ca^{2+}, SO_4^{2-}, and H_2O)

[30] The following discussion concerning the geochemistry needed to form the observed gypsum is based upon the available information to date about the composition of the north polar dune sea and the polar layered deposits. Studies dedicated to thorough, detailed compositional mapping of the entirety of this particular dune sea have not yet been performed, making it extremely difficult to build a comprehensive chemical/thermodynamical model concerning the formation pathways of gypsum. This discussion is thus, at this point, somewhat speculative.

[31] Throughout this section, we assume that the water, which has emanated from the polar deposits, is pure because the exact composition of the polar deposits is unknown and because Mars Express Mars Advanced Radar for Subsurface and Ionosphere Sounding (MARSIS) data imply a nearly 100% water composition [*Plaut et al.*, 2006]. Note that if any dust (which likely contains sulfates [*Hamilton et al.*, 2005]) was present in the water, it would not have increased the acidity of the water. Regardless, sulfate has not been detected by OMEGA within the polar deposits, indicating that it is likely present in only minor amounts if at all.

3.2.1. Sulfur

[32] Generally, the sulfate deposits observed on Mars are attributed to the following two possible origins: alteration in the presence of SO_2 [*Fairen et al.*, 2004; *Tosca et al.*, 2004] and alteration in the presence of sulfides (like pyrrhotite) [*Burns and Fisher*, 1990b; *Burns*, 1993]. The first origin implies dissolution in water of SO_2 produced by volcanic activity [*Postawko and Kuhn*, 1986; *Waenke et al.*, 1992]. The resulting strong acid (H_2SO_4) can easily alter surrounding silicates. However, the source of SO_2 must be relatively close to the sulfate deposit since the high reactivity of H_2SO_4 implies fast kinetics of alteration and sulfate precipitation.

[33] The second origin implies the concomitant weathering of silicates and sulfides in the presence of water, in oxidative conditions. Previous experiments have demonstrated that alteration of diopside and pyrrhotite in a simulated Martian atmosphere produces mostly Fe sulfates but also produces gypsum in small amounts; as soon as even trace amounts of calcium come in contact with sulfur, gypsum precipitates [*Chevrier et al.*, 2004, 2006]. This hypothesis presents an advantage in simplicity in that a nearby volcanic source is not required; only sulfide, water, and calcium are required. Similarity of some Martian meteorites and primary rocks with terrestrial komatiites has long suggested the possible presence of abundant sulfides in the Martian crust [*Clark and Baird*, 1979; *Burns and Fisher*, 1990a]. In addition, sulfides are two to three times more abundant in SNC shergottites than in their

terrestrial equivalents [*Lorand et al.*, 2005]. The evolution of these sulfides in oxidative conditions is hypothesized to have led to sulfate deposits, such as jarosite or gypsum, at various places on Mars [*Burns and Fisher*, 1990b, 1993]. The presence of sulfide in the Olympia Undae dunes would provide a ready source of local sulfur without needing to invoke late Amazonian volcanism.

[34] It should be noted that, while the ubiquitous, Martian dust does contain sulfur (and hence could be considered as a sulfur source), that sulfur is inferred, for the most part, to already be in the form of sulfates [*Hamilton et al.*, 2005]. Therefore dust could not be the source of the sulfur for a gypsum deposit containing no other sulfates unless all of the sulfate within the dust were gypsum, which is not thought to be the case. Additionally, since sulfates are stable on the surface of Mars, there is no particular reason to assume that the dust would destabilize to form a gypsum deposit.

3.2.2. Calcium

[35] Identifying possible sources of calcium is a bit trickier. Considering the primary mineralogy identified on Mars, the main potential source of Ca^{2+} is clinopyroxene (high-calcium pyroxene (HCP), $Ca(Mg, Fe)Si_2O_6$) which is widely distributed on the surface of Mars (according to OMEGA observations) [*Bibring et al.*, 2005; *Mustard et al.*, 2005]. HCP is present in minor amounts at various locations within the north polar region, including near and within the sand sea (Figure 1c). An important issue in considering HCP as a calcium source is the behavior of primary iron and magnesium within the HCP. The Fe^{3+} ion forms easily from Fe^{2+} present in primary phases and is extremely insoluble under high-oxidation levels and moderate acidity ($pH \geq \sim 3$). In the case of this gypsum deposit, the necessary presence of SO_4^{2-} in the water indicates high-oxidation levels, but the pH of the water is unknown; we will assume, for the purposes of this discussion, that the pH was above 3. If the primary pyroxene contained iron, iron oxides (any evolved crystalline product from the precipitation of ferrihydrite $\sim Fe(OH)_3$, which includes hematite, Fe_2O_3, goethite, FeO(OH), and magnetite, Fe_3O_4) or even Fe-bearing sulfates (jarosite) should be present as secondary phases [*Sracek et al.*, 2004]. OMEGA observations infer the presence of a dark, spectrally featureless (DSF) phase mixed with the gypsum, a description which can be attributed to an oxide. Using inclusions of oxide as darkening agents in the gypsum grains not only provides an excellent fit to our compositional model, as explained in section 2.1, but is also consistent with alteration of Fe-rich HCP.

[36] The case for Mg^{2+} is different. Alteration of Mg-bearing HCP forms rather soluble salts, such as kieserite, also observed on Mars within Valles Marineris [*Gendrin et al.*, 2005]. Thus, if the primary HCP contained magnesium but not iron, it is more likely that spatial fractionation of minerals would occur and that gypsum would precipitate first (closest to the water source) while more soluble Mg-rich salts would be carried further by the water. In the case of in situ alteration, gypsum would precipitate first and the more soluble salts later, on top of or near the gypsum, but not mixed with it. Nevertheless, no Mg sulfate deposit has been observed close to the gypsum dunes.

[37] Alteration of wollastonite ($CaSiO_3$) or anorthite ($CaAl_2Si_2O_8$), instead of HCP, can form gypsum alone with no associated secondary phases (except for silica, SiO_2). Considering the high content of magnesium and iron on the Martian surface, alteration of wollastonite or anorthite remains less likely than alteration of HCP. Yet, the observation of quartzofeldspathic minerals in the northern plains [*Banfield et al.*, 2004] suggests that evolved materials enriched in alkaline elements are present on Mars, even if apparently disconnected (at the surface at least) from the northern gypsum deposits. Andesine-labradorite is present within TES surface types I and II [*Bandfield et al.*, 2000] and could also serve as a calcium source. However, if the gypsum within the dunes was created in situ (see section 3.3), then the aluminum must have also remained within the dunes, forming secondary phases which have thus far not been observed. Note that plagioclase itself cannot be detected by OMEGA.

[38] Of these possibilities, the most likely source of calcium appears to be Fe-bearing HCP. HCP has been identified within and near the Olympia Undae dune field, as well as in many other locations on Mars, and the oxides which would result as secondary phases might well be the dark inclusions we suggest exist within most of the gypsum grains.

3.2.3. Water

[39] Since gypsum is a soft mineral, it cannot saltate long distances. Thus one would expect the gypsum source region to lie close to or within the highest gypsum concentrations. As shown in the map in Figure 1 and in the close-up in Figure 12, sinuous valleys extending from the polar cap terminate just to the east of the high-gypsum area. We hypothesize that the most likely origin of these valleys is fluvial erosion resulting from the melting and outflow event which most likely initiated the formation of Chasma Boreale to the east [*Fishbaugh and Head*, 2002]. An alternate or additional water source could be melting due to the formation of the nearby impact crater in the PLD. Note in Figure 12a that small amounts of gypsum (associated with dunes) surround the region where the channels terminate. Currently, younger, higher-albedo material (likely ice/frost and dust) covers this area (Figure 12c), masking the signature of any gypsum potentially existing within it. The proximity of these channels and the highest concentrations of gypsum implies a causal relationship.

[40] Having identified the chemistry needed to produce the gypsum within the limits of what is currently known about the composition of the polar dune field, the question now becomes, ''What was the depositional environment of the gypsum?''.

3.3. Possible Depositional Environments

[41] Evaporite deposits form when salt minerals precipitate out of evaporating saline water. This process can occur in several main types of depositional environments: lacustrine, fluvial, eolian, springs, and saline soils [*Smoot and Lowenstein*, 1991]. While evaporative processes may often involve leaching of Ca by acidic water and transport of dissolved salts to another location where the evaporation occurs, this situation is unlikely for the Martian north polar deposits. Liquid may not be able to remain stable at the surface long enough to allow distant transport.

3.3.1. Lacustrine

[42] The largest terrestrial gypsum deposits typically form in closed basins. As different minerals precipitate

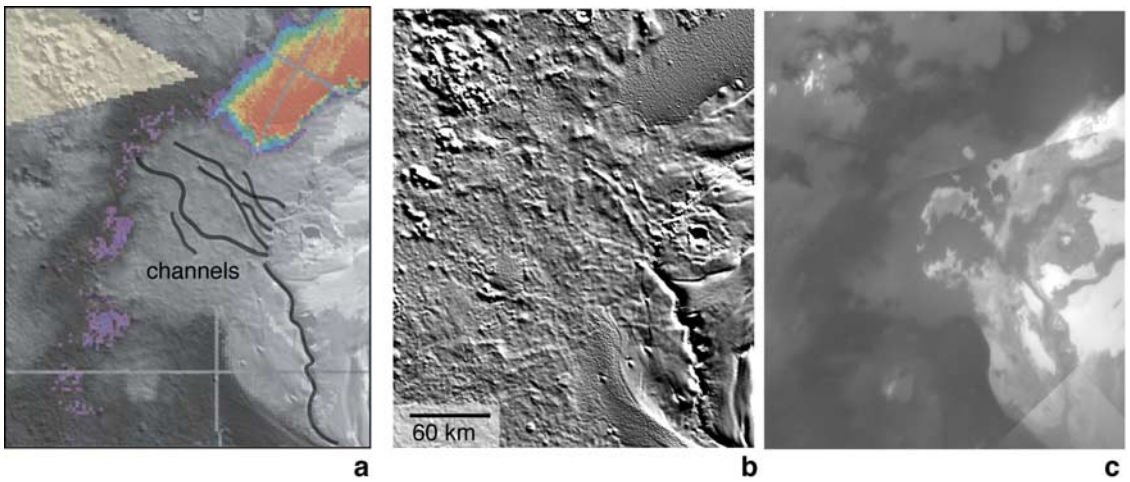

Figure 12. (a) Close-up of the gypsum source region. See Figure 1 for context. (b) MOLA-shaded relief of same area. (c) Portion of MOC wide-angle mosaic. Valleys visible in the MOLA data are outlined in Figure 12a. We interpret the valleys as channels formed by outflow of water either from the Chasma Boreale melting event [*Fishbaugh and Head*, 2002] or by melting due to the nearby impact into the polar cap. Note that the area around the channels has a slightly higher albedo in the MOC mosaic resulting from a cover of frost/ice and dust.

out of standing water enclosed in the basin, the water chemistry changes, creating a sequence of mineral formation wherein the most soluble minerals precipitate last. Classically, this can translate into the development of different layers of salt, with the bottom layer consisting of the least-soluble mineral. Usually, carbonates will precipitate before gypsum, but *Catling* [1999] has theorized that gypsum may form early, if not first, in an evaporite sequence on Mars if $SO_4^{2-}/Ca^{2+} > 2$ and if the atmospheric partial pressure of CO_2 is greater than 3 bar. Such a situation could possibly account for the almost complete lack of other salts in association with the polar gypsum deposit. However, we cannot know what the particular value of SO_4^{2-}/Ca^{2+} is in the case of the Martian north polar gypsum, and the associated atmospheric pressure is 500× greater than the current pressure. Additionally, there is no evidence for a basin outside the current margin of the polar cap unless it has since been modified by deposition or erosion or it has since been covered by southward extension of the PLD margin.

[43] On the other hand, saline mudflats, a lacustrine subenvironment, do not necessarily require an obvious basin [*Smoot and Lowenstein*, 1991]. These mudflats consist of fine-grained sediment which comes into contact, perhaps intermittently, with saline water. In this environment, salt minerals grow within the sediment by evaporation, forming layers of salt, aggregates of crystals, or individual crystals which can incorporate grains of other material. Commonly, saline mudflats are covered in crusts of relatively insoluble minerals, like gypsum. Salts may also form in dry mudflats [*Smoot and Lowenstein*, 1991] that come into contact with even less water, but the quantity produced is even smaller than in saline mudflats. Perhaps the area surrounding the channel mouths served as such a mudflat. The largest obstacle to this scenario is the fact that all of the observed gypsum is now incorporated into dunes. So where is the original evaporite deposit, unless it is undetectable due to the dust/ice/frost covering the channel mouth region (as stated in section 3.2.3 and seen in Figure 12)?

[44] We find a lacustrine origin to be unsatisfactory because it is difficult to either prove or disprove. We can find no evidence of an evaporite basin or of a gypsum source deposit, even if there are various scenarios that could explain this lack of evidence.

3.3.2. Fluvial

[45] In terrestrial fluvial environments with the appropriate geochemistry, one may find evaporites at the toe of an alluvial fan, in abandoned stream meanders, and in floodplains (which are really a saline soil environment, see section 3.3.5) [*Smoot and Lowenstein*, 1991]. In all cases but the floodplain, the amount of evaporitic material produced is small and not always euhedral (i.e., does not always have a fully developed crystal form), often forming crusts; such a scenario is not conducive to eventual incorporation into dunes, nor is it consistent with the large amount of gypsum observed in the Martian polar dune sea.

3.3.3. Eolian

[46] Evaporites may also form in terrestrial interdune spaces that intermittently host saline groundwater or act as playas [*Smoot and Lowenstein*, 1991]. In this type of environment, the evaporites will form crusts or even crystals which sometimes grow around sand grains. If such a processes had taken place within the Olympia Undae dune sea, then we would expect almost the entirety of the observed gypsum to exist within the interdune spaces, making these areas brighter than the dunes themselves. As explained in section 2.2.1, bright patches do exist in interdune areas, but they are not ubiquitous, and are small in total area compared to the dunes themselves.

3.3.4. Springs

[47] Saline springs may also produce evaporites. We will not discuss this possibility in detail here since we have no particular reason to call upon groundwater being brought to

the surface by hydrostatic pressure when we have already identified a more obvious water conduit, the channels. Invoking spring activity adds unnecessary complexity to the story. From where did the groundwater come, and why was this putative groundwater under hydrostatic pressure?

3.3.5. Saline Soils

[48] If saline water percolates downward through soil, evaporites could develop within the pore spaces, with gypsum and halite being the most common such evaporites in terrestrial soils [*Smoot and Lowenstein*, 1991]. Euhedral crystals can form in this environment and may even poikilitically trap soil grains within them.

[49] We can translate this environment to the Olympia Undae dune field on Mars. Water emptied from the channels to the east. Some of this water entered the eastern margin of the polar dune sea nearby. Since the dunes themselves contained Ca-rich pyroxene and sulfide, the dune grains were altered into gypsum as water encasing the grains evaporated; additionally, evaporative gypsum crystals were created in the pore spaces as the water percolated through the dunes. Whether or not direct alteration of the materials just beyond the channel mouths occurred is unknown since younger materials cover this area. In any case, alteration of loose sand grains would take place more easily than alteration of other deposits, given the large surface area involved. In both direct alteration of basaltic sand and in formation of evaporative gypsum crystals, dark basaltic grains could easily end up encased within the gypsum grains, lowering their albedo. As explained in section 3.2, dark oxide inclusions, produced as secondary phases, would also darken the grains and are implied to exist by our compositional modeling. In situ alteration of dune material and creation of evaporative gypsum crystals by percolation of water delivered from nearby channels through the dunes provide a simple explanation of the creation of this unique gypsum deposit in an environment unique to this location. Water, sulfur, calcium, and easily alterable sand grains are provided locally, without the need to bring materials from outside the region of the north PLD, without the need to invoke large-scale, distant volcanic activity to provide hydrothermal circulation or sulfur, and without requiring an explanation for the lack of evidence for an evaporite basin or for a primary evaporite deposit. However, while this hypothesis best follows Occam's Razor, several important issues remain.

3.4. Further Analysis and Open Questions

3.4.1. Amounts and Rates

[50] Given the many uncertainties involved, it is extremely difficult to calculate how much calcium, sulfur, and water were required to form the amount of gypsum observed, how long the weathering process took, or even to estimate errors in any such calculations. However, here, we attempt first-order estimates of these values. We first make a rough estimate of the volume of dune material within the high-gypsum area by breaking up this area into rectangles to calculate the surface area ($\sim$7500 km^2), as shown in Figure 13a. We then assume that the typical elevation variations of 10 m, as observed in a profile of MOLA gridded data across the area (Figure 13b), represent the thickness of dune deposits and that the regional slope along the profile is due to subdune topography (for example, hidden layers of the basal unit). Hence this is a conservative volume estimate. The resulting volume of dunes corresponding to the area of highest gypsum concentration (red in Figure 1a) is $\sim$75 km^3. In all of the calculations below we assume that the concentrations of gypsum calculated in section 2.1 are representative of the entire 75-km^3 volume.

[51] Assuming a porosity of the dunes of 66% and a composition of 100% gypsum (thus ignoring the volume taken up by dark inclusions within the gypsum grains), we get 25 km^3 (5.8×10^{13} kg) of pure crystalline gypsum. This mass of gypsum corresponds to a mass of CaO of 1.9×10^{13} kg. If all Martian basalts contain 10 wt.% CaO, as they do at Gusev [*Gellert et al.*, 2004], then one needs 1.9×10^{14} kg of basaltic material. If all of the necessary sulfur comes from sulfide, then since 1 mol of Ca^{2+} must react with 1 mol of SO_4^{2-}, 2.9×10^{13} kg of sulfide is required. However, if the typical amount of sulfide in Martian basalts is equivalent to the 0.5 wt.% value in shergottites [*Lorand et al.*, 2005], then only 9.5×10^{11} kg of sulfide would be present in our 1.9×10^{14} kg of basaltic material, a factor of 30 too little. Obviously, large uncertainties on the amounts of CaO or sulfur in Martian basalts can modify this rough calculation. For instance, increasing the amount of sulfur in the basalts by a factor 10 to be in better agreement with the amount of sulfur found in Martian soils by in situ measurement [*Yen et al.*, 2005] could provide enough sulfur to explain the amount of gypsum.

[52] If the 0.5 wt.% value for sulfide in basalts is correct, then it is possible that alteration of basaltic material alone could not produce the amount of gypsum observed. We are left with three explanations. First, the alteration process consumed all of the calcium, and an excess of sulfur was present from, for example, a hidden sulfide deposit, an enrichment of sulfide in the basal unit which is the source for most (if not all) of the dunes, and/or a nearby volcanic eruption. While volcanic features have been noted near the region of Chasma Boreale mouth [*Hodges and Moore*, 1994; *Garvin et al.*, 2000], their age is unknown, and their connection to this gypsum deposit cannot be definitively established. The presence of a large hidden sulfide source (for example, komatiitic rocks) or enrichment of the basal unit in sulfide cannot be proven. Second, all of the sulfide was consumed in the presence of an excess of calcium, requiring even more basaltic material (and hence more magnesium and iron) and the consequent likely presence of secondary mineral phases (like Mg and Fe sulfates). Such secondary phases have not been observed, so that, if this scenario is the case, these minerals must have left the system, given their higher solubility. Third, the amount of gypsum observed by OMEGA is not typical of the entire bulk volume of dune deposits in which it is observed.

[53] Mass balance issues concerning the sulfide also remain to be solved. Sulfide will liberate SO_4 into solution, but it will also liberate Fe, so one may expect to see Fe sulfates in association with the gypsum. Such sulfates have not been observed. Some of this mass balance problem can be solved if the DSF phase within the gypsum is magnetite. Magnetite is one of the oxides expected as a secondary phase in the alteration of basaltic material, and it can act as a geochemical sink for the Fe. Even with an equal starting amount of Fe and S, the resulting gypsum/magnetite ratio will be $\sim$10. Since the reflectance properties of the dune

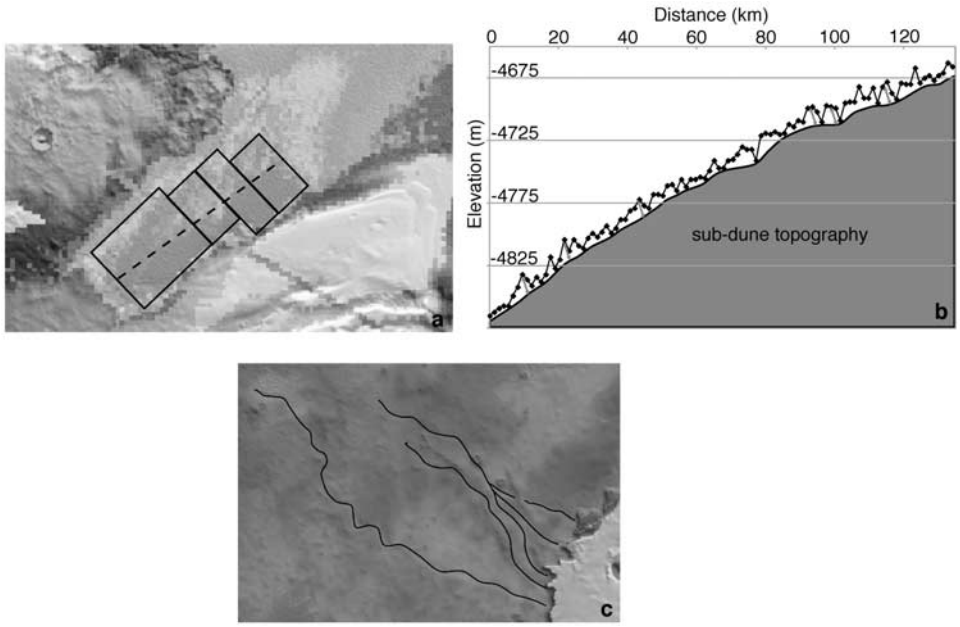

Figure 13. (a) Portion of the map in Figure 1a showing eastern edge of dune sea in black and white. Boxes indicate rectangles used for calculating surface area of the high-gypsum area. Dashed line shows location of MOLA profile in Figure 13b. (b) Profile of MOLA gridded data through high-gypsum area of dunes. Thickness of dune deposit is taken to be magnitude of topography variation (as indicated by grey arrows), ignoring regional slope. This thickness is about 10 m. (c) Close-up of channels outlined in Figure 12. Black lines indicate channel lengths used in calculation of the amount of water delivered by the channels. Gray scale MOLA topography over MOLA-shaded relief. Other than the polar cap margin exposed in the lower right corner, lower elevations are darker. Channels are each ~10 m deep.

material are largely sensitive to the volume ratios of the components, magnetite would effectively hide the "missing" iron.

[54] On the basis of the hydration of gypsum, an absolute minimum amount of requisite water is 6×10^{12} kg (60 km^3). Estimating the amount of water delivered by the nearby channels for comparison is not straightforward. We cannot know how many outflow events occurred or by how much subsequent geologic activity has altered their morphology (for example, by burying portions of the channels). The best estimate that we can obtain of water delivered is to calculate the volume of currently visible channels (as outlined in Figure 13) using MOLA data. This volume comes to only 12 km^3. Thus some of the channels have been infilled, the channels were filled more than once (up to ~5 times), most of the water was delivered by the long, sinuous channel connecting these smaller channels to the Chasma Boreale region, and/or, again, the amount of gypsum observed is not typical of the bulk dune deposits in the gypsum-rich area.

[55] Finally, we come to the timing. Previous experiments have shown that sulfates can form within 1 year [*Chevrier et al.*, 2004, 2006]. Therefore, in the case of weathering in the presence of SO_2 or of sulfides, the formation process of gypsum could be relatively fast compared to geologic timescales. Exact numbers for this particular gypsum deposit are impossible to calculate. Clearly, the water needed to have remained liquid long enough to form the gypsum. The question of how long the water needed to remain liquid is nearly impossible to calculate. Speculatively, we suggest that the dune material acted as a kinetic barrier and the dissolved salts as a chemical barrier to evaporation while the water was circulating within the dunes. Of course, this brings up the further question of exactly how, physically, the water circulated within the dunes, something which is beyond the scope of this paper but can be examined in detail in a future study.

3.4.2. What About Chasma Boreale?

[56] If melting of the PLD initiated the formation of Chasma Boreale [*Clifford*, 1987; *Benito et al.*, 1997; *Fishbaugh and Head*, 2002], then why is gypsum present in only extremely minor amounts in the Chasma Boreale region? OMEGA data indicate only trace amounts of gypsum within the chasma (Figure 14), and the presence of bright patches that may be composed of gypsum (section 3.1) within the dune patch bordering the mesa beyond the Chasma mouth.

[57] Several factors may have precluded the formation or detection of gypsum here. As described above, formation of detectable amounts of gypsum by direct alteration of mafic materials will most easily take place where a deposit of loose grains exists (for example, a dune field), and dunes may also be needed to slow the evaporation process enough to allow formation of significant quantities of evaporitic grains. *Fishbaugh and Head* [2002] postulated that when the formation of Chasma Boreale was initiated by melting, water initially flowed beneath the ice. There is not necessarily any reason to believe that sediment deposits or dune fields existed beneath the ice at that time. Additionally, any gypsum which did form could have been redissolved or mechanically broken down during transport. Finally, eolian

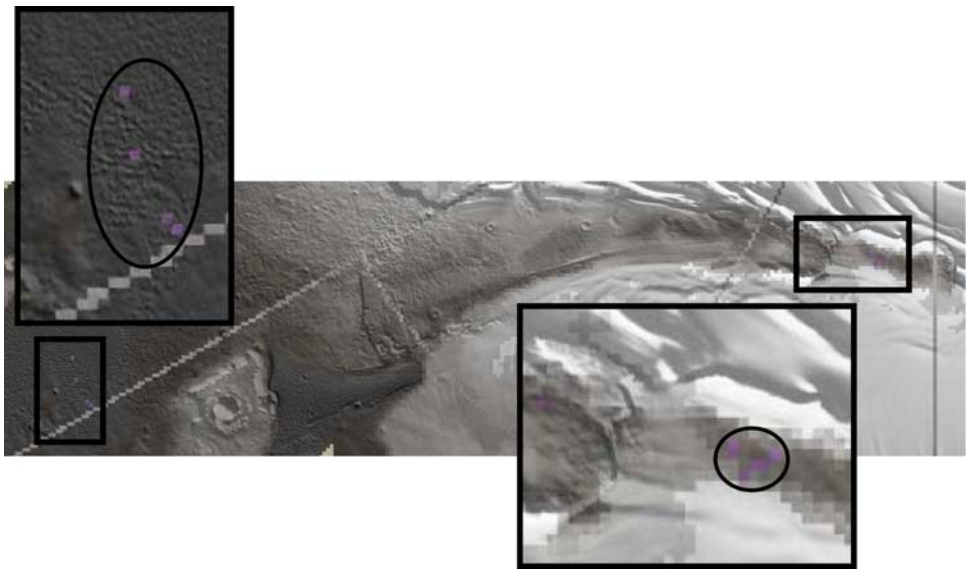

Figure 14. Part of OMEGA gypsum concentration map overlain on MOLA-shaded relief showing close-up of Chasma Boreale region. Even when contrast enhanced, gypsum concentrations in this region appear minor to nonexistent on this map. Band depth scale is the same as in Figure 1a.

erosion and deposition within the Chasma since its formation has certainly affected its present appearance [*Howard*, 2000; *Fishbaugh and Head*, 2002], possibly stripping away some of any meltwater-related deposits.

4. Conclusions

[58] OMEGA has detected gypsum in the north polar region only within the Olympia Undae sand sea and a few nearby, isolated dune patches, not within the circumpolar materials, PLD, or basal unit. In the most gypsum-rich areas, the best fit to our compositional model yields concentrations of 35% pure gypsum grains of a few tens of microns in size mixed with 65% millimeter-sized gypsum grains containing inclusions of a dark, spectrally featureless material. Eolian-rippled, bright patches (distinguished from bright patches of underlying material), observed in MOC images between dunes and scattered throughout the gypsum-bearing area, might account for the fine-grained, pure gypsum and for the mechanical break down of gypsum during saltation; but preliminary CRISM observations indicate lower gypsum concentrations in these patches compared to the dunes themselves. No morphological, significant average albedo, color, or temperature anomalies manifest themselves within the gypsum-rich dunes.

[59] We propose that water from nearby channels percolated through the eastern end of the Olympia Undae dune sea. The gypsum most likely formed as a result of the creation of evaporative gypsum grains and of direct alteration of sand dune grains bearing high-calcium, Fe-rich pyroxene and sulfide. Such alteration would produce oxide as a secondary phase; secondary oxides, such as magnetite, could easily act as the spectrally featureless darkening agent (the inclusions) implied by our compositional modeling to exist within the gypsum grains. Creation of evaporative crystals could easily involve trapping of basaltic grains within them which would also lower the albedo of the crystals.

[60] Liquid water was produced by the Chasma Boreale melting event and/or by melting due to the nearby impact into ice. The presence of a large expanse of dune material (which can be easily altered and which provides plenty of pore space in which evaporative crystals can grow) near the mouths of meltwater channels conspired to create a unique situation wherein gypsum was able to form on Mars, even within the late Amazonian. No distant volcanic activity is required, and the confined distribution of the gypsum is easily explained by this hypothesis. An evaporative deposit (similar to those created in saline mudflats or on alluvial fans) may exist near the channel mouths, but its existence is impossible to prove with orbital spectrometer data since this area is now covered by dust and frost/ice.

[61] Rough estimates, based on geochemistry, of the amount of sulfur and calcium required to form the amount of gypsum observed indicate that roughly 30 times more sulfide could be needed than what likely exists within the dunes. Although we are aware that these calculations are based on values with large uncertainties, we propose that the possible ‘‘missing sulfide’’ could stem from the fact that the estimated concentration of gypsum detected by OMEGA does not represent the concentration within the entire three-dimensional volume of dune material in which it is found. More complex explanations include the presence of a hidden sulfide source, late Amazonian volcanism as a supply of sulfur, or enrichment of sulfide in the basal unit (the source for most, if not all, of the dunes, but not of the gypsum).

[62] Dedicated observations of the Olympia Undae dunes by CRISM could shed even more detailed light on the north polar gypsum story. One may be able to assess the composition of small-scale structures such as small collections of the rippled, the bright patches observed within some dunes, and hills and knobs within and near these dunes which may

contain or be blanketed by gypsum. Detailed compositional mapping of the dune field would also be a key step in the building of a more thorough understanding of the geochemical pathways taken by the gypsum. Another future step of this analysis could consist of initiating a study using OMEGA results to complement those of thermal instruments, MGS TES and Odyssey THEMIS, sensitive to non-Fe-bearing minerals.

[63] **Acknowledgments.** Josh Bandfield (Arizona State University) and Nicolas Tosca (SUNY Stony Brook) provided thorough, constructive reviews which improved the quality of this paper. The authors wish to thank the staff of THMPROC (Arizona State University), especially Josh Bandfield, and the USGS for crucial help in processing THEMIS data and importing data into ESRI Arcmap. Patrick Russell (University of Bern) also provided helpful comments.

References

Arvidson, R., F. Poulet, J.-P. Bibring, M. Wolff, A. Gendrin, R. Morris, J. Freeman, Y. Langevin, N. Mangold, and G. Bellucci (2005), Spectral reflectance and morphologic correlations in Eastern Terra Meridiani, Mars, *Science*, *307*(5715), 1576–1581.

Bandfield, J. (2002), Global mineral distributions on Mars, *J. Geophys. Res.*, *107*(E6), 5042, doi:10.1029/2001JE001510.

Bandfield, J., V. Hamilton, and P. Christensen (2000), A global view of Martian surface compositions from MGS-TES, *Science*, *287*, 1626–1630.

Banfield, J., V. Hamilton, and H. McSween (2004), Identification of quartzofeldspathic materials on Mars, *J. Geophys. Res.*, *109*, E10009, doi:10.1029/2004JE002290.

Benito, G., F. Mediavilla, M. Fernandez, A. Marquez, J. Martinez, and F. Anguita (1997), Chasma Boreale, Mars: A sapping and outflow channel with a tectono-thermal origin, *Icarus*, *129*, 528–538.

Bibring, J.-P., et al. (2005), Mars surface diversity as revealed by the OMEGA/Mars Express observations, *Science*, *307*, 1576–1581.

Bibring, J.-P., et al. (2006), Global mineralogical and aqueous Mars history derived from OMEGA/Mars Express data, *Science*, *312 5772*, 400–404.

Burns, R. (1993), Rates and mechanisms of chemical weathering of ferromagnesian silicate minerals on Mars, *Geochim. Cosmochim. Acta*, *57*, 4555–4574.

Burns, R., and D. Fisher (1990a), Evolution of sulfide mineralization on Mars, *J. Geophys. Res.*, *95*(B9), 14,169–14,173.

Burns, R., and D. Fisher (1990b), Iron-sulfur mineralogy of Mars: Magmatic evolution and chemical weathering products, *J. Geophys. Res.*, *95*(B9), 14,415–14,421.

Burns, R., and D. Fisher (1993), Rates of oxidative weathering on the surface of Mars, *J. Geophys. Res.*, *98*(E2), 3365–3372.

Byrne, S., and B. Murray (2002), North polar stratigraphy and the paleo-erg of Mars, *J. Geophys. Res.*, *107*(E6), 5044, doi:10.1029/2001JE001615.

Carr, M. (1996), *Water on Mars*, 229 pp., Oxford Univ. Press, New York.

Catling, D. (1999), A chemical model for evaporites on early Mars: Possible sedimentary tracers of the early climate and implications for exploration, *J. Geophys. Res.*, *104*(E07), 16,453–16,470.

Chevrier, V., P. Rochette, P.-E. Mathé, and O. Grauby (2004), Weathering of iron-rich phases in simulated Martian atmospheres, *Geology*, *32*(12), 1033–1036.

Chevrier, V., P. Mathé, P. Rochette, O. Grauby, G. Bourrie, and F. Trolard (2006), Iron weathering products in a CO_2 + (H_2O or H_2O_2) atmosphere: Implications for weathering processes on the surface of Mars, *Geochim. Cosmochim. Acta*, *70*, 4295–4317.

Christansen, E. (1989), Lahars in the Elysium region of Mars, *Geology*, *17*, 203–206.

Christensen, P. R., et al. (2003), Morphology and composition of the surface of Mars: Mars Odyssey THEMIS results, *Science*, *300*(5628), 2056–2061.

Clark, B., and A. Baird (1979), Is the Martian lithosphere sulfur rich?, *J. Geophys. Res.*, *84*(B14), 8395–8403.

Clark, R., G. Swayze, A. Gallagher, T. King, and W. Calvin (1993), U.S. Geological Survey Digital spectral library version 1: 0.2 to 3.0 microns, *U.S. Geol. Surv. Open File Rep. 93–592*, http://speclab.cr.usgs.gov.

Clifford, S. (1987), Polar basal melting on Mars, *J. Geophys. Res.*, *92*, 9135–9152.

Edgett, K., and P. Christensen (1991), The particle size of Martian eolian dunes, *J. Geophys. Res.*, *96*(E5), 22,765–22,776.

Edgett, K., and M. Malin (2000), New views of Mars eolian activity, materials, and surface properties: Three vignettes from the Mars Global Surveyor Camera, *J. Geophys. Res.*, *105*(E1), 1623–1650.

Edgett, K., R. Williams, M. Malin, B. Cantor, and P. Thomas (2003), Mars landscape evolution: Influence of stratigraphy on geomorphology in the north polar region, *Geomorphology*, *52*, 289–297.

Fairen, A., D. Fernandez-Remolar, J. Dohm, V. Baker, and R. Amils (2004), Inhibition of carbonate synthesis in acidic oceans on early Mars, *Nature*, *431*, 423–426.

Fishbaugh, K. (2005), Characterization of Martian north polar geologic units using Mars Odyssey THEMIS data, paper presented at *Lunar and Planetary Science Conference* 36, Lunar and Planetary Institute, Houston, Abstract 1335.

Fishbaugh, K., and J. Head (2002), Chasma Boreale, Mars: Topographic characterization from Mars Orbiter Laser Altimeter data and implications for mechanisms of formation, *J. Geophys. Res.*, *107*(E3), 5013, doi:10.1029/2000JE001351.

Fishbaugh, K., and J. Head (2005), Origin and characteristics of the Mars north polar basal unit and implications for polar geologic history, *Icarus*, *174*(2), 444–474.

Garvin, J., S. Sakimoto, J. Frawley, C. Schnetzler, and H. Wright (2000), Topographic evidence for geologically recent near-polar volcanism on Mars, *Icarus*, *145*(2), 648–652.

Gellert, R., et al. (2004), Chemistry of rocks and soils in Gusev Crater from the Alpha Particle X-ray Spectrometer, *Science*, *305*(5685), 829–832.

Gendrin, A., et al. (2005), Sulfates in Martian layered terrains: The OMEGA/Mars Express view, *Science*, *307*, 1587–1591.

Hamilton, V., H. McSween, and B. Hapke (2005), Mineralogy of Martian atmospheric dust inferred from thermal infrared spectra of aerosols, *J. Geophys. Res.*, *110*, E12006, doi:10.1029/2005JE002501.

Hapke, B. (1981), Bidirectional reflectance spectroscopy: 1. Theory, *J. Geophys. Res.*, *86*, 4571–4586.

Hartmann, W., and G. Neukum (2001), Cratering chronology and the evolution of Mars, in *Chronology and Evolution of Mars*, edited by R. Kallenbach and A. Vasavada (1999), Dark material in the polar layered deposits and dunes on Mars, *J. Geophys. Res.*, *104*(E7), 16,487–16,500.

Herkenhoff, K., and A. Vasavada (1999), Dark material in the polar layered deposits and dunes on Mars, *J. Geophys. Res.*, *104*(E7), 16,487–416,500.

Hodges, C., and H. Moore (1994), Atlas of volcanic landforms on Mars, *U.S. Geol. Surv. Prof. Pap.*, 1534.

Howard, A. (2000), The role of eolian processes in forming surface features of the Martian polar layered deposits, *Icarus*, *144*, 267–288.

Langevin, Y., F. Poulet, J.-P. Bibring, and B. Gondet (2005), Sulfates in the north polar region of Mars detected by OMEGA/Mars Express, *Science*, *307*(5715), 1584–1586.

Langford, R. (2003), The Holocene history of the White Sands dune field and influences on eolian deflation and playa lakes, *Quat. Int.*, *104*(1), 31–39.

Lee, P., and P. Thomas (1995), Longitudinal dunes on Mars: Relation to current wind regime, *J. Geophys. Res.*, *100*(E3), 5381–5395.

Lorand, J., V. Chevrier, and V. Sautter (2005), Sulfide mineralogy and redox conditions in some shergottites, *Meteorit. Planet. Sci.*, *40*(8), 1257–1272.

Malin, M., and K. Edgett (2000), Evidence for recent groundwater seepage and surface runoff on Mars, *Science*, *288*(5475), 2230–2335.

Martinez-Frías, J., R. Lunar, J. Rodríguez-Losada, A. Delgado, and F. Rull (2004), The volcanism-related multistage hydrothermal system of El Jaroso (SE Spain): Implications for the exploration of Mars, *Earth Planets Space*, *56*(7), v–viii.

McKee, E. (1966), Structures of dunes at White Sands National Monument, New Mexico (and comparison with structures of dunes from other selected areas), *Sedimentology*, *7*, 1–69.

Ming, D., et al. (2004), Geochemical and mineralogical indicators for aqueous processes in the Columbia Hills of Gusev crater, Mars, *J. Geophys. Res.*, *111*, E02S12, doi:10.1029/2005JE002560.

Mustard, J., F. Poulet, A. Gendrin, J.-P. Bibring, Y. Langevin, B. Gondet, N. Mangold, G. Bellucci, and F. Altieri (2005), Olivine and pyroxene diversity in the crust of Mars, *Science*, *307*, 1594–1597.

Paige, D., J. Bachman, and K. Keegan (1994), Thermal and albedo mapping of the polar regions of Mars using Viking thermal mapper observations: 1. North polar region, *J. Geophys. Res.*, *99*(E12), 25,991–925,959.

Plaut, J., et al. (2006), MARSIS Subsurface Sounding Observations of the Polar Deposits of Mars, paper presented, *Eos Trans. AGU*, *87*(52), Fall Meet. Suppl., Abstract P13-D06.

Postawko, S., and W. Kuhn (1986), Effect of greenhouse gases (CO_2, H_2O, SO_2) on Martian paleoclimate, *J. Geophys. Res.*, *91*(B4), D431–D438.

Poulet, F., and S. Erard (2004), Nonlinear spectral mixing: Quantitative analysis of laboratory mineral mixtures, *J. Geophys. Res.*, *109*, E02009, doi:10.1029/2003JE002179.

Poulet, F., N. Mangold, and S. Erard (2003), A new view of dark Martian regions from geomorphic and spectroscopic analysis of Syrtis Major, *Astron. Astrophys.*, *412*, L19–L23.

Poulet, F., J.-P. Bibring, J. Mustard, A. Gendrin, N. Mangold, Y. Langevin, R. Arvidson, B. Gondet, and C. Gomez (2005a), Phyllosilicates on Mars and implications for the Early Mars History, *Nature*, *481*, 623–627.

Poulet, F., Y. Langevin, J. P. Bibring, B. Gondet, R. Arvidson, and T. O. Team (2005b), Mineralogy of the northern high latitude regions of Mars, paper presented at *Lunar and Planetary Science Conference* 36, Lunar and Planetary Institute, Houston, Abstract 1828.

Poulet, F., C. Gomez, J.-P. Bibring, Y. Langevin, B. Gondet, P. Pinet, G. Belluci, J. Mustard, and the OMEGA team (2007), Martian surface mineralogy from OMEGA/MEx: Global mineral maps, *J. Geophys. Res.*, doi:10. 1029/2006JE002840, in press.

Reider, R., et al. (2004), Chemistry of rocks and soils at Meridiani Planum from the alpha particle X-ray spectrometer, *Science*, *306*, 1746–1749.

Roush, T., F. Esposito, G. Rossman, and L. Colangeli (2006), Gypsum optical constants in the visible and near-infrared: Real and imagined, paper presented at *Lunar and Planetary Science Conference* 37, Lunar and Planetary Science Institute, Houston, TX, Abstract 1188.

Russell, P., and J. Head (2003), Elysium-Utopia flows as mega-lahars: A model of dike intrusion, cryosphere cracking, and water-sediment release, *J. Geophys. Res.*, *108*(E6), 5064, doi:10.1029/2002JE001995.

Schatz, V., H. Tsoar, K. Edgett, E. Parteli, and H. Herrmann (2006), Evidence for indurated sand dunes in the Martian north polar region, *J. Geophys. Res.*, *111*, E04006, doi:10.1029/2005JE002514.

Shkuratov, Y., L. Starukhina, H. Hoffmann, and G. Arnold (1999), A model of spectral albedo of particulate surfaces: Implications for optical properties of the Moon, *Icarus*, *137*, 235–246.

Sinha, R., and B. Raymahashay (2004), Evaporite mineralogy and geochemical evolution of the Sambhar Salt Lake, Rajasthan, India, *Sediment. Geol.*, *166*, 59–71.

Skinner, J., and K. Tanaka (2001), Regional emplacement history of the Utopia and Elysium plains deposits, paper presented at *Lunar and Planetary Science Conference* 32, Lunar and Planetary Science Institute, Houston, Abstract 2154.

Smoot, J., and T. Lowenstein (1991), Depositional environments of nonmarine evaporites, in *Evaporites, Petroleum, and Mineral Resources*, edited by J. Melvin et al., pp. 165–196, Springer, New York.

Squyres, S. W., et al. (2004), In situ evidence for an ancient aqueous environment at Meridiani Planum, Mars, *Science*, *306*, 1709–1714.

Sracek, O., M. Choquette, P. Gelina, F. Lefebvre, and R. Nicholson (2004), Geochemical characterization of acid mine drainage from a waste rock pile, Mine Doyon, Quebec, Canada, *J. Contam. Hydro.*, *69*, 45–71.

Tanaka, K. (2006), Mars' north polar gypsum: Possible origin related to early Amazonian magmatism at Alba Patera and aeolian mining, paper presented at *Fourth International Mars Polar Science and Exploration Conference*, Lunar and Planetary Science Institute, Davos, Switzerland, Abstract 8024.

Tanaka, K., and D. McKinnon (1989), Release of Martian catastrophic floods by fracture discharge from volcanotectonic regions, paper presented at *4th International Conference on Mars*, Univ. of Ariz. Press, Tucson.

Tanaka, K., J. Skinner, and T. Hare (2005), Geologic map of the northern plains of Mars, *U.S. Geol. Surv., Sci. Invest. Ser., Map 288*.

Thomas, P., and C. Weitz (1989), Sand dune materials and polar layered deposits on Mars, *Icarus*, *81*, 185–215.

Thomas, P., et al. (1999), Bright dunes on Mars, *Nature*, *397*, 592–594.

Tosca, N. J., and S. M. McLennan (2005), Evaporites at Meridiani Planum and implications for surficial processes on Mars, *Eos Trans. AGU*, *86*(52), Fall Meet. Suppl. Abstract P12A-07.

Tosca, N., A. McLennan, D. Lindsley, and M. Schoonen (2004), Acid-sulfate weathering of synthetic Martian basalt: The acid fog model revisited, *J. Geophys. Res.*, *109*, E05003, doi:10.1029/2003JE002218.

Tosca, N., S. McLennan, B. Clark, J. Grotzinger, J. Hurowitz, A. Knoll, C. Shroeder, and S. Squyres (2005), Geochemical modeling of evaporation processes on Mars: Insight from the sedimentary record at Meridiani Planum, *Earth Planet. Sci. Lett.*, *240*, 122–148.

Tsoar, H., R. Greeley, and A. Peterfreund (1979), Mars: The north polar sand sea and related wind patterns, *J. Geophys. Res.*, *84*(B14), 8167–8180.

Vysotskiy, E., A. Makhnach, T. Peryt, and S. Kruchek (2004), Marine and continental Lower Permian evaporites of the Prypiac' Trough (Belarus), *Sediment. Geol.*, *172*, 211–222.

Waenke, H., G. Driebus, E. Jagoutz, and L. Mukhin (1992), Volatiles on Mars: The role of SO2, paper presented at *Lunar and Planetary Science Conference* 23, Lunar and Planetary Science Institute, Houston, TX, Abstract, 1489–1490.

Yen, A., et al. (2005), An integrated view of the chemistry and mineralogy of Martian soils, *Nature*, *436*, 49–54.

J.-P. Bibring, Y. Langevin, and F. Poulet, Institut d'Astrophysique Spatiale, Université Paris-Sud XI, Orsay, France.

V. Chevrier, W. M. Keck Laboratory for Space and Planetary Simulations, MUSE 202, University of Arkansas, Fayetteville, AR 72701, USA.

K. E. Fishbaugh, International Space Science Institute, Hallerstrasse 6, CH-3012, Bern, Switzerland. (fishbaugh@issibern.ch)